Gemeda *et al.*
Journal of Engineering and Applied Science (2024) 71:146
https://doi.org/10.1186/s44147-024-00427-5

Journal of Engineering and Applied Science

RESEARCH Open Access

Multi-objective parametric optimization process of hybrid reinforced titanium metal matrix composite through Taguchi-Grey relation analysis (TGRA)

Birhane Assefa Gemeda[1], Devendra Kumar Sinha[1*], Getinet Asrat Mengesha[2] and Satyam Shivam Gautam[3]

*Correspondence:
ds3621781@gmail.com;
devendrasinhame@gmail.com

[1] Mechanical Engineering Department, School of Mechnaical, Chemical and Materials Engineering Center of Excellence Advanced Manufcaturing Engineering, Adama Science & Technology University, Adama City, Ethiopia
[2] Materials Science and Engineering department, School of Mechanical, Chemical and Materials Engineering, Adama Science & Technology University, Adama City, Ethiopia
[3] Department Mechanical Engineering, North Eastern Regional Institute of Science and Technology, Itanagar, Arunachal Pradesh 791109, India

Abstract

Hybrid titanium metal matrix composites (HTMMCs) are advanced composite materials that can be tailored to a variety of applications. Because of their decreased fuel consumption and cost, they are popular in the transportation industry. Using multi-objective optimization and Taguchi-based Grey relational analysis (TGRA), this study investigates the impact of hybrid reinforced HTMMCs synthesized using powder metallurgy on their physic mechanical properties. The research investigates reinforcements such as B_4C, SiC, ZrO_2, and MoS_2 at various compaction pressures, milling durations, and sintering temperatures. The best powder metallurgy control parameters for HTMMC synthesis, with a milling time of 5 h, a compaction pressure of 40 MPa, a sintering temperature of 1200 °C, and a sintering time of 1 h, and a compaction time of 40 min. According to validation results, HTMMC material with optimized process parameters had experimental densities, porosities, hardness, compressive strength, and wear rates of 4.29 gm/cm^3, 0.1178%, 71.53RHN, 2782.36 MPa, and 0.1519 mm^3 correspondingly. The material hardness was increased by 1.99% and compressive strength by 2.87%. The use of Taguchi and GRA techniques strongly verified that the impact of milling duration and sintering temperature was the greatest of all five factors. The novel synthesized hybrid reinforcing HTMMCs outperformed pure Ti grade 5 and single and double fortified HTMMCs in terms of physic mechanical characteristics. As a result, the newly developed tetra hybrid reinforced HTMMC material is expected to be used in heavy-duty vehicles, aerospace, automobiles, maritime, and other industries.

Highlights

- Developed new HTMMCs engineering material using powder metallurgy.
- In a multi-response optimization process, Taguchi-based Grey relational analysis (TGRA) was used to determine the most effective combinations of process variables.
- The high relative density, robust interface, and minimal cavities/porosity (less than 1%) of the sintered specimens make them acceptable engineering materials for use in the automotive and aerospace industries.

- The optimized HTMMC material exhibited improved hardness and compressive strength examination results, with an improvement of 1.99% in hardness and 2.87% in compressive strength.

Keywords: Titanium, Reinforcements, Nanoparticle, Powder metallurgy, Multi-objective optimization

Introduction

Metal Matrix Composites (MMCs) are important in a variety of sectors due to their strength, low weight, and resistance to wear and corrosion. They are widely used in the automotive and aviation sectors because of their reliability and durability, minimal carbon emissions, and good mechanical qualities. MMCs also minimize energy/fuel consumption, manufacturing costs, and industrial waste [1].

Titanium is a popular and sophisticated engineering material due to its low density, biocompatibility, and high strength, but it poses production issues due to its limited wear resistance, high price, and brittle nature. Researchers are studying thermomechanical methods to minimize manufacturing costs while increasing performance, with the ultimate goal of creating titanium and its alloys at cheap prices, notably in transportation, by employing nanoparticles as a new ultrafine reinforcing material [2, 3].

Pure titanium grade 5 is currently the most desirable metallic material for aerospace applications due to its low density (4.43 g/cm^3), high strength-to-density ratio, and exceptional corrosion resistance. Titanium and its alloys exhibit poor wear resistance [4, 5] are difficult to manufacture into useable products and machines [2], and are prohibitively expensive [6]. Titanium oxide is formed at all processing temperatures, and its concentration is mostly determined by temperature. The oxide layer, made of TiO_2, generates a multi-layered porous structure with linear oxidation kinetics. Titanium's oxygen affinity causes it to react with oxygen in the air, generating a TiO_2 layer on the surface that shields the substrate from further oxidation and corrosion in a variety of hostile situations [7].

Titanium is brittle and readily broken down at ambient temperature, but it may be reinforced using thermomechanical processes like substitution and interstitial addition. Its mechanical qualities are restricted, rendering it ineffective for mechanical applications. Temperature influences its behavior, with brittleness at room temperature and ductility at higher degrees [3, 8].

Titanium metal matrix composites (TMMCs) are popular because of their exceptional combination of mechanical and physical qualities, such as enhanced strength, low weight, high stiffness, amazing elastic modulus, great strength-to-weight ratio, and high wear resistance. These composite materials are made by integrating two or more materials to improve mechanical qualities such as tribological, structural, thermal, wear, chemical, and corrosion resistance [9, 10]. Composite combinations and amalgamations provide superior properties [11].

Numerous forms of particles, whiskers, or fiber ceramics including Ti_5Si_3 [12], SiC [13], TiO_2 [14], graphene nanoplatelet [15], nanodiamonds [16], TiB_2 and WC [17], ZrO_2 [18], B_4C [19], MoS_2 [20], and rare earth oxides like La_2O_3 [21] and Nd_2O_3 [22]

were all recommended previously to improve the properties of TMMCs. According to scholars [23], the type of reinforcement utilized is determined by the intended use of the material and industry demand. Because of their enhanced coefficient of friction, corrosion and wear resistance, hardness, yield, tensile strength, and robustness performance, B_4C, SiC, MoS_2, and ZrO_2 are considered to be desirable reinforcements for titanium matrix.

Traditional methods like squeeze casting, stir casting, spray casting, and compo casting are used to create composites [24]. When compared to machining, casting, and forging with Powder Metallurgy (PM), PM is an energy-saving, environmentally friendly advance that allows for more complex shapes. PM is vital for the mass manufacture of automotive components because it has better yield strength, tensile strength, compressive strength, and elongation than casting parts. PM consists of three operations: milling, compaction, and sintering. Milling introduces mixed particles and sizing, compaction processes combine powder particles to a green body, and sintering methods encourage and enhance amalgamation and densification [25].

Recent research investigates several methodologies for creating monolithic/hybrid reinforcements in multi-modulus composites (MMCs), including Taguchi, ANOVA, response surface approach, full factorial, and DOE [26, 27]. The constraints of single-objective optimization, which is frequently employed for TMMCs, are that it only offers the most appropriate process parameters. By determining the optimal input parameter value, multi-objective optimization addresses all major objectives [28]. The paper suggests that porosity, wear rate, and density be reduced while compressive strength and hardness be increased. Temperature, particle size, compaction pressure, and particle concentration may all be adjusted to optimize outcomes. The density, porosity, hardness, compression strength, and tensile toughness of synthesized hybrid reinforcement MMCs were investigated using the TGRA technique [29].

The current study is focused on the development of Hybrid Titanium Metal Matrix Composites (HTMMCs) with superior physical and mechanical properties by mixing SiC, ZrO_2, MoS_2, and B_4C ceramics to pure Ti grade 5 matrixes. Additionally, to optimize the physic mechanical properties, control components such as powder metallurgical process parameters and hybrid reinforcement weight percentage were adjusted using Taguchi and GRA approaches.

Methods

Chemical composition of reinforcement and matrix in hybrid TMMC synthesis

Powder metallurgy (PM) is used in the study to generate nanocomposites of grade 5 titanium, B_4C, SiC, MoS_2, and ZrO_2 nanoparticles with sizes of 90–100 nm, purity > 99%, and reinforcement purity of 99% acquired from Saveer Matrix Nano Pvt. Ltd., Uttar Pradesh, India. The study looks at the mechanical properties of powder metallurgy-based processes for producing particle-reinforced MMCs, with an emphasis on powder blending, mixing, cold compression, and sintering.

Particulate-reinforced composites (SiC, B4C, ZrO2, and MoS2) are cheaper than fiber-reinforced composites, and the physical, mechanical, tribological, and corrosion properties of particles are frequently isotropic [30, 31]. This study uses four different types of particles as reinforcing materials, with MoS2 potentially self-lubricating. Hybrid

reinforcements outperform other reinforcements in terms of performance, cost, and weight reduction while improving material properties [32].

Synthesis and characterization HTMMCS

The researchers used pressure-less sintering to manufacture Ti-B_4C, MoS_2 SiC, and ZrO_2 nanocomposites and investigated their mechanical properties such as microstructure, density, hardness, wear rate, and reinforced dimensions dependency and dispersion. The powder blend was made by combining grade 5 Ti powder with nanoparticle fortification of these powders. Sintered samples were 10.0 mm in diameter and 12 mm in height.

The materials' morphology was investigated using a Model JCM/6000Plus Bench Top SEM and the elemental phases present in the manufactured samples were analyzed using XRD in accordance with the XRD working principle: Bragg's law the XRD was performed on a fully computerized powder X-ray diffractometer (XRD7000 X-ray diffractometer, Shimadzu Corporation (Japan)) at 40 kV and 30 mA. The compressive strength was investigated using a Universal Testing Machine (UTM) model Bairo electro computer-controlled-hydraulic universal testing machine type HUT-600 from Beijing United Tester Co., Ltd., Beijing, China. A Digital Rockwell micro-hardness type HRS-150, Beijing United Tester Co., Ltd. of Beijing, China, was also used for micro-hardness measuring device testing, with a weight of 150 kgf and a holding time of 15 s. Archimedes' method was applied to test specimens to approximate their porosity, bulk density, actual density, and water absorption. The sintered weight of the specimen was first determined using a precision digital weighing balance (HR-250AZ, A&D Company Limited, Korea) with a 0.0001-gm accuracy.

HTMMCs were created using powder metallurgy, and the wear rate was measured using a pin-on-disc device. Tribological analysis and investigation were done under dry conditions, a 6-mm diameter and 12 mm height specimen was slid against an EN31 steel disc of 120 mm diameter and 65 HRC hardness utilizing POD equipment in accordance with ASTM: G 99 standards utilized DUCOM-TR-20 Micro model (Bangalore, India, DUCOM Instruments Company Pvt. Ltd.) Every specimen was subjected to additional tests with varying loads (10, 20, 30N) and sliding velocity (4,4.5, 5 m/s). Fig. 1 depicts the methodological design for the evaluation and characterization of the synthesis's HTMMCs.

Powder metallurgy production method

The PM technique is a cost-effective way of making near-net particle-reinforced MMCs that provides adaptability, lower production costs, and less scrapping waste [32]. By ensuring homogeneous reinforcing material dispersion by powder mixing, compaction, and sintering, PM processing enhances mechanical characteristics while preventing clustering. The earlier published paper [33] describes the steps of the PM manufacturing procedure in depth.

DOE utilizes the Taguchi approach

The Taguchi methodology is an optimization method that uses a modified L27 orthogonal array and is measured using the signal-to-noise ratio (S/N). It focuses

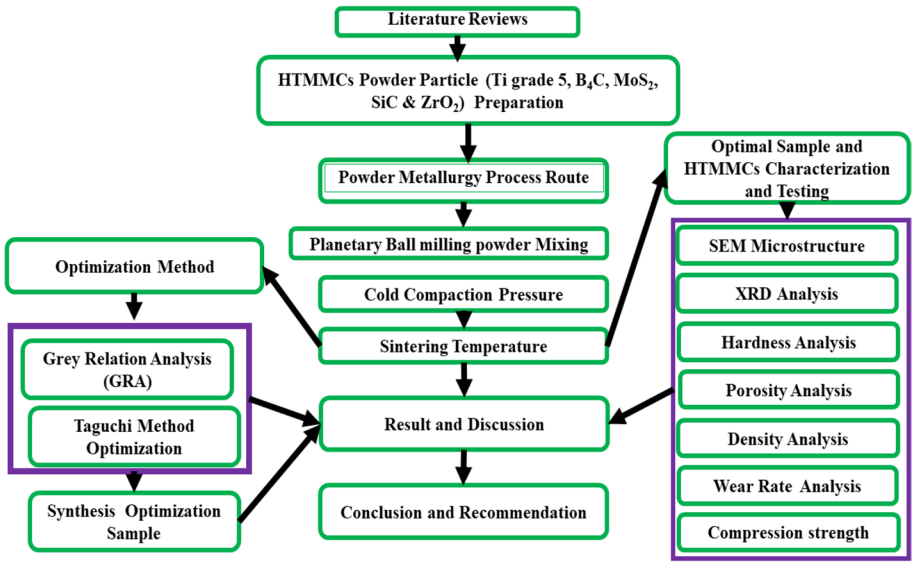

Fig. 1 HTMMCs synthetization and optimization methodology flow diagram

Table 1 Process and reinforcement factors and their levels

S. N	TMCs optimization process parameters	Unit	Parameters designation	Level		
				1	2	3
1	Milling duration	H	MD	4	5	6
2	Compaction pressure	MPa	CP	40	45	50
3	Compaction duration	Min	CD	30	40	50
4	Sintering temperature	^0C	ST	800	1000	1200
5	Sintering duration	Hrs	SD	1	1.5	2
6	MoS_2 Wt.%	Wt.%	MoS_2	4	4	4
7	SiC Wt.%	Wt.%	SiC	2.5	5	7.5
8	B_4C Wt.%	Wt.%	B_4C	2.5	5	7.5
9	ZrO_2 Wt.%	Wt.%	ZrO_2	2.5	5	7.5

on reducing repetitions and obtaining the greatest results as rapidly as possible. The experimental trial, which included 27 trials, was modeled using Minitab Statistical Software. Quality is measured by the S/N, which quantifies communication and engineering application efficiency. Depending on the needed features, upgrades, and applications, lower or higher values imply higher quality. Table 1 describes the experiment's process and reinforcement parts, as well as their quantities, as well as their specified variables and levels.

The selection of reinforcement weight percentage was made based on the most desirable outcome from a prior inquiry, the reputation of consistent mechanical qualities in various scholars' analyzed works, and extra enhancement of mechanical and physical properties. Moreover, the upper and lower levels of each parameter were selected based on the literature available in the field of study.

Previous study reveals that MoS_2 addition in a Ti metal matrix by 4%, yielded the best results which are compatible with the findings of many scholars' investigations.

Table 2 List of L27 OA experimental designs

S. N	Milling time	Compaction pressure	Compaction time	Sintering temperature	Sintering time	SiC	B_4C	ZrO_2	MoS_2
	(h)	(MPa)	(min)	(°C)	(h)	%	%	%	%
1	4	40	30	800	1	2.5	2.5	2.5	4
2	4	40	30	800	1.5	5	5	5	4
3	4	40	30	800	2	7.5	7.5	7.5	4
4	4	45	40	1000	1	2.5	2.5	5	4
5	4	45	40	1000	1.5	5	5	7.5	4
6	4	45	40	1000	2	7.5	7.5	2.5	4
7	4	50	50	1200	1	2.5	2.5	7.5	4
8	4	50	50	1200	1.5	5	5	2.5	4
9	4	50	50	1200	2	7.5	7.5	5	4
10	5	40	40	1200	1	5	7.5	2.5	4
11	5	40	40	1200	1.5	7.5	5	7.5	4
12	5	40	40	1200	2	2.5	5	7.5	4
13	5	45	50	800	1	5	7.5	5	4
14	5	45	50	800	1.5	7.5	2.5	7.5	4
15	5	45	50	800	2	2.5	5	2.5	4
16	5	50	30	1000	1	5	7.5	7.5	4
17	5	50	30	1000	1.5	7.5	2.5	2.5	4
18	5	50	30	1000	2	2.5	5	5	4
19	6	40	50	1000	1	7.5	5	2.5	4
20	6	40	50	1000	1.5	2.5	7.5	5	4
21	6	40	50	1000	2	5	2.5	7.5	4
22	6	45	30	1200	1	7.5	5	5	4
23	6	45	30	1200	1.5	2.5	7.5	7.5	4
24	6	45	30	1200	2	5	2.5	2.5	4
25	6	50	40	800	1	7.5	2.5	5	4
26	6	50	40	800	1.5	2.5	7.5	2.5	4
27	6	50	40	800	2	5	2.5	5	4

In this manuscript, therefore weight percentage of MoS2 is fixed at 4% for all specimen preparations.

Additionally in detailed list of experimentation trial L27 OA is shown in Table 2, where L27 signifies the maximum number of rows (experimentation trial repetition).

Grey relation analysis (GRA)

GRA outperforms other approaches due to its capacity to assess partial and restricted data while preserving trust and it's one of the most effective approaches [34]. The Grey relational grade (GRG) is an approach that uses DOE considerations to examine data and determine the relevance of items in research. It ranks the evaluated features based on specified scores or ratings, highlighting the most important ones [35]. In one research, GRA was utilized to examine densities, wear rates, porosities, hardness, and compressive strength in 27 sets of examinations. Fig. 2 depicts the calculation of the ideal variable level configurations for multiple responses of synthesized HTM-MCs material.

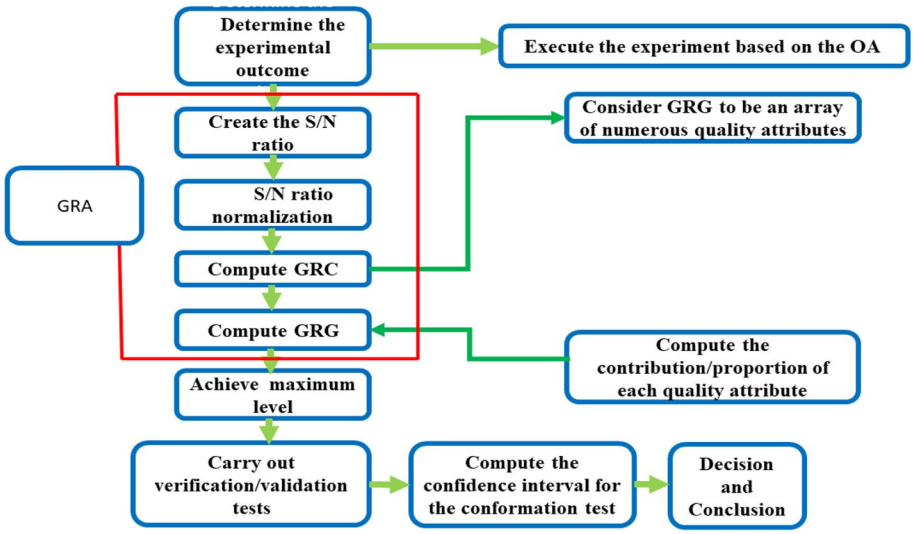

Fig. 2 Development of synthesized HTMMCS optimization flow diagram

Results and discussion

Data from experimentally measured results

In a multi-response optimization process, Taguchi-based Grey relational analysis (TGRA) was utilized to discover the most successful combinations of process variables [36]. GRA was utilized for matrix analysis and the approach was employed for experiment design and execution. The findings revealed that raising desirable quality characteristics and S/N enhanced performance, consequently improving product design, manufacturing process, and system effectiveness. Table 3 illustrates the observed response statistics from the experiment findings. The GRG estimation approach merged many physic mechanical domain results into a single standard database, with the highest GRG score value deemed critical. The GRG is calculated for each data combination in order to find the most significant factors, resulting in better outcomes.

Multi-response optimized performance of stages within GRA

Taguchi's approach is used to find the best process parameter configurations for a given set of attributes. For several responses with various quality features, multi-response optimization utilizing GRA is advised [37]. The goal of this research was to find the best process parameter combination for lowering wear rate, porosity, and enhancing Rockwell microhardness type "C" and compressive strength. The method creates a GRG for measuring the degree of connection of several responses, merging various performance criteria into a single Grey relationship grade. Table 4 shows the S/N (η) ratio for the calculated values. The following stages are investigated for GRA.

Stage 1: Convert original experimental result data into S/N ratio (η) using applicable formulae for quality characteristics, defining the larger the better-quality ratios using Eq. (1), and three for compression strength replications and eight for Rockwell hardness type "C" tests.

Table 3 Observed response statistics from the experiment findings

S. N	Smaller is the higher-quality differentiating feature						Larger is the higher-quality differentiating feature									
	Porosity (P) (%)			Sliding wear rate (WR)(mm^3)			Compressi ve strength (CS) (MPa)			Rockwell type "C" hardness analysis (H)(HRC)						
	P-1	P-2	P-3	WR-1	WR-2	WR-3	CS-1	CS-2	CS-3	H-1	H-2	H-3	H-4	H-5	H-6	H-7	H-8
1	0.41	0.39	0.43	0.216	0.2	0.083	1568	1552	1537	45.15	39.62	44.25	39.13	43.52	37.82	42.66	37.36
2	0.5	0.48	0.53	0.216	0.2	0.083	1625	1609	1593	46.73	41.01	45.79	40.49	45.03	39.14	44.15	38.66
3	0.43	0.41	0.45	0.217	0.201	0.084	1479	1464	1450	42.53	37.32	41.68	36.86	40.9	35.62	40.18	35.19
4	0.4	0.38	0.42	0.215	0.199	0.083	1688	1671	1654	48.3	42.39	47.34	41.86	46.55	40.46	45.64	39.97
5	0.26	0.24	0.27	0.213	0.197	0.082	2392	2368	2344	59.85	52.53	58.65	51.87	57.68	50.13	56.55	49.52
6	0.34	0.33	0.36	0.214	0.198	0.083	2148	2127	2105	54.6	47.92	53.51	47.32	52.62	45.73	51.59	45.18
7	0.34	0.32	0.35	0.214	0.198	0.082	2208	2186	2164	55.65	48.84	54.54	48.23	53.64	46.61	52.58	46.05
8	0.39	0.37	0.41	0.215	0.199	0.083	1790	1772	1754	50.4	44.23	49.39	43.68	48.58	42.22	47.62	41.7
9	0.38	0.36	0.4	0.214	0.198	0.083	1950	1930	1911	52.5	46.08	51.45	45.5	50.6	43.98	49.61	43.44
10	0.28	0.27	0.3	0.213	0.197	0.082	2327	2303	2281	57.75	50.68	56.59	50.05	55.66	48.37	54.57	47.79
11	0.13	0.12	0.13	0.212	0.196	0.082	2627	2600	2574	63	55.29	61.74	54.6	60.72	52.77	59.53	52.13
12	0.16	0.16	0.17	0.212	0.197	0.082	2432	2408	2388	61.43	53.91	60.19	53.24	59.2	51.45	58.04	50.83
13	0.39	0.37	0.41	0.216	0.2	0.084	1560	1544	1529	44.1	38.7	43.22	38.22	42.5	36.94	41.67	36.49
14	0.51	0.49	0.54	0.217	0.201	0.084	1508	1493	1478	43.05	37.78	42.19	37.31	41.49	36.06	40.68	35.62
15	0.45	0.43	0.48	0.218	0.201	0.084	1307	1294	1281	39.9	35.02	39.1	34.58	38.46	33.42	37.7	33.02
16	0.16	0.15	0.17	0.212	0.196	0.082	2520	2494	2470	61.95	54.37	60.71	53.69	59.71	51.89	58.54	51.26
17	0.35	0.34	0.37	0.215	0.199	0.083	1875	1856	1837	51.45	45.15	50.42	44.59	49.59	43.09	48.62	42.57
18	0.44	0.42	0.46	0.214	0.198	0.083	2025	2005	1985	53.55	46.99	52.48	46.41	51.61	44.86	50.59	44.31
19	0.37	0.35	0.39	0.215	0.199	0.083	1760	1742	1724	49.35	43.31	48.36	42.77	47.56	41.34	46.63	40.84
20	0.35	0.33	0.37	0.215	0.199	0.083	1840	1821	1803	50.93	44.69	49.91	44.14	49.08	42.66	48.12	42.14

Table 3 (continued)

S. N	Smaller is the higher-quality differentiating feature						Larger is the higher-quality differentiating feature										
	Porosity (P) (%)			Sliding wear rate (WR)(mm^3)			Compressi ve strength (CS) (MPa)			Rockwell type "C" hardness analysis (H)(HRC)							
	P-1	P-2	P-3	WR-1	WR-2	WR-3	CS-1	CS-2	CS-3	H-1	H-2	H-3	H-4	H-5	H-6	H-7	H-8
21	0.44	0.42	0.46	0.216	0.2	0.083	1629	1613	1597	47.25	41.47	46.31	40.95	45.54	39.58	44.65	39.09
22	0.17	0.16	0.18	0.213	0.197	0.082	2425	2400	2377	60.9	53.45	59.68	52.78	58.69	51.01	57.54	50.39
23	0.3	0.28	0.31	0.213	0.198	0.082	2250	2228	2205	56.7	49.76	55.57	49.14	54.65	47.49	53.58	46.92
24	0.26	0.25	0.28	0.213	0.197	0.082	2340	2316	2293	58.8	51.6	57.62	50.96	56.67	49.25	55.56	48.66
25	0.4	0.38	0.42	0.217	0.201	0.084	1357	1343	1330	40.95	35.94	40.13	35.49	39.47	34.3	38.69	33.88
26	0.42	0.4	0.44	0.216	0.2	0.083	1603	1587	1571	46.2	40.55	45.28	40.04	44.53	38.69	43.65	38.23
27	0.47	0.44	0.49	0.217	0.201	0.084	1439	1425	1410	42	36.86	41.16	36.4	40.48	35.18	39.69	34.75

Table 4 The ratio S/N (η) for the determined values

S. N	The smaller the better		The greater is better	
	Ratio of S/N of (P)	Ratio of S/N of (WR)	Ratio of S/N of (CS)	Ratio of S/N of (H)
1	7.7374	15.0502	63.8188	32.2329
2	5.9556	15.0684	64.1302	32.5336
3	7.3243	15.0247	63.3119	31.7134
4	7.9515	15.0854	64.4586	32.8149
5	11.8023	15.1907	67.4867	34.6852
6	9.2799	15.1464	66.553	33.8827
7	9.45	15.1551	66.7921	34.045
8	8.171	15.1025	64.9683	33.1875
9	8.3963	15.1294	65.7117	33.5457
10	10.9456	15.1715	67.2475	34.3651
11	17.9406	15.2245	68.2996	35.1286
12	15.7348	15.2081	67.6372	34.9079
13	8.171	15.0417	63.7739	32.0273
14	5.785	15.0331	63.4803	31.8177
15	6.8624	14.9981	62.2378	31.1577
16	15.9062	15.2166	67.9393	34.9757
17	9.0308	15.1188	65.3706	33.3629
18	7.1249	15.1379	66.0414	33.7161
19	8.6275	15.0939	64.82	33.0016
20	9.1091	15.1111	65.2068	33.279
21	7.1249	15.0768	64.1518	32.628
22	15.3809	15.1994	67.6057	34.828
23	10.5469	15.1636	66.9561	34.2136
24	15.5801	15.1801	67.3419	34.5222
25	7.9515	15.0058	62.5628	31.3846
26	7.5284	15.0587	64.0106	32.4336
27	6.6114	15.0142	63.0733	31.6052

$$\frac{S}{N}(\eta) = -10Log\left[\frac{1}{m}\sum_{i=1}^{m}\frac{1}{Xi^2}\right] \tag{1}$$

whereas m is the number of replication tests performed and xi had a response that was values that were measured.

To convert the S/N ratio, use Eq. (2) and three repeats of each response, with smaller responses better desirable for porosity and wear rate.

$$\frac{S}{N}(\eta) = -10Log\left[\frac{1}{m}\sum_{i=1}^{m}Xi^2\right] \tag{2}$$

The subsequent S/N ratio for generated outcomes is calculated in a resembling manner using the applicable Eqs. (1) and (2) provided and shown in Table 3.

Stage 2: Normalize ηij as Zij ($0 \le Zij \le 1$) using Eqs. (4) and (5) to reduce variance and avoid using various units. Using a Grey relational generating strategy, Taguchi's method provides normalized S/N ratios between 0 and 1 [37]. Greater values

maximize compressive strength and Rockwell microhardness, whereas lower values reduce MMC porosity [38].

Normalization of the S/N ratio is accomplished using Eq. (3), with bigger being better.

$$\mathrm{Zij} = \frac{\mathrm{nij} - \mathrm{Min(nij)}}{\mathrm{Max\left(nij\right)} - \mathrm{Min(nij)}} \tag{3}$$

Normalization is accomplished using the formula (4) given below to calculate S/N ratios, where the lower the value scale the better.

$$\mathrm{Zij} = \frac{\mathrm{Max\left(nij\right)} - \mathrm{nij}}{\mathrm{Max\left(nij\right)} - \mathrm{Min(nij)}} \tag{4}$$

where Zij is the normalized value for the *i*th experiment for the *j*th dependent factor/response, ηij is the S/N ratio to be normalized, and max (ηij) and min(ηij) are the maximum and minimum values of ηij, correspondingly.

Table 5 Computed normalized S/N ratios of determined results

S. N	S/N ratios normalized (η) for lower is better		S/N ratios normalized (η) for higher is better	
	S/N ratio of (P)	S/N ratio of (WR)	S/N ratio of (CS)	S/N ratio of (H)
1	1	1	1	1
2	0.167363191	0.034893993	0.940562209	0.961494875
3	0.181463688	0.072438163	0.890725527	0.94442066
4	0.194190332	0.110865724	0.885529051	0.924299277
5	0.210577841	0.149293286	0.865897918	0.888337656
6	0.50497713	0.196113074	0.842010624	0.847289028
7	0.575454934	0.23409894	0.826437692	0.807726208
8	0.608254632	0.268992933	0.778366162	0.769573648
9	0.698492876	0.306537102	0.751311492	0.72711476
10	0.712486426	0.344964664	0.711867762	0.686242414
11	0.726537563	0.382508834	0.627470388	0.644287189
12	0.732979038	0.420053004	0.573080603	0.601375003
13	0.766157162	0.466872792	0.516810188	0.555340099
14	0.785177202	0.500883392	0.489788512	0.534211388
15	0.803711869	0.538869258	0.450443763	0.511168753
16	0.803711869	0.576855124	0.425979082	0.464353169
17	0.82176939	0.614399293	0.366359827	0.41733612
18	0.82176939	0.652385159	0.315747798	0.370268705
19	0.839382671	0.689487633	0.3121845	0.346495757
20	0.856576393	0.732332155	0.292454386	0.321312549
21	0.873367008	0.769876325	0.26081362	0.270769851
22	0.88977097	0.807420495	0.253406579	0.218993175
23	0.88977097	0.84540636	0.20497212	0.166209172
re24	0.911365955	0.882508834	0.177191593	0.139943086
25	0.932014874	0.928886926	0.137830347	0.112694855
26	0.985965316	0.965989399	0.053614438	0.057140699
27	1	1	0	0

Table 6 Deviation series progression for normalized S/N ratios (η)

S. no	Deviation series (Δij have the exact same equation expression)			
	ΔP	**ΔWR**	**ΔCS**	**ΔH**
1	0	0	0	0
2	0.832636809	0.965106007	0.059437791	0.038505125
3	0.818536312	0.927561837	0.109274473	0.05557934
4	0.805809668	0.889134276	0.114470949	0.075700723
5	0.789422159	0.850706714	0.134102082	0.111662344
6	0.49502287	0.803886926	0.157989376	0.152710972
7	0.424545066	0.76590106	0.173562308	0.192273792
8	0.391745368	0.731007067	0.221633838	0.230426352
9	0.301507124	0.693462898	0.248688508	0.27288524
10	0.287513574	0.655035336	0.288132238	0.313757586
11	0.273462437	0.617491166	0.372529612	0.355712811
12	0.267020962	0.579946996	0.426919397	0.398624997
13	0.233842838	0.533127208	0.483189812	0.444659901
14	0.214822798	0.499116608	0.510211488	0.465788612
15	0.196288131	0.461130742	0.549556237	0.488831247
16	0.196288131	0.423144876	0.574020918	0.535646831
17	0.17823061	0.385600707	0.633640173	0.58266388
18	0.17823061	0.347614841	0.684252202	0.629731295
19	0.160617329	0.310512367	0.6878155	0.653504243
20	0.143423607	0.267667845	0.707545614	0.678687451
21	0.126632992	0.230123675	0.73918638	0.729230149
22	0.11022903	0.192579505	0.746593421	0.781006825
23	0.11022903	0.15459364	0.79502788	0.833790828
24	0.088634045	0.117491166	0.822808407	0.860056914
25	0.067985126	0.071113074	0.862169653	0.887305145
26	0.014034684	0.034010601	0.946385562	0.942859301
27	0	0	1	1

Based on Julong's [39] investigation, larger normalized results equate to higher achievement, and the optimal normalized outcome should equal one. The GRC is then calculated to indicate the relationship between ideal (best) and actual examination outcomes. Table 5 figured out normalized S/N ratios of determined results computed from Table 4 calculated data utilized the above-mentioned formulae (3) and (4).

Stage 3. The computation of the deviation sequences ((Δij) in both quality characteristics is identical, and the equation is as follows; Δ = absolute difference between Zij^0 and Zij, which is a variation from the desired level and may be considered a quality loss. Table 6 shows the Deviation sequence for the various normalized S/N ratios (η) as Eq. (5).

$$\Delta ij = Zij^{0^\circ} -^\circ Zij \tag{5}$$

whereas Δij denotes the deviation series and Zij^0 is typically equal to one ($Zij^0 = 1$).

Stage 4: Computation of GRCs calculation: The following equation is used to calculate the GRC for normalized S/N ratio data.

Table 7 Grey relational grades (GRGs) and Grey relational coefficients (GRCs)

S. N	Grey relational coefficients (GRCs)				Grey relational grades (GRGs)
	P	WR	CS	H	
1	1	1	1	1	1
2	0.545661854	0.5088784	0.943896856	0.962922547	0.740339914
3	0.549892786	0.518790101	0.90149014	0.947347075	0.729380026
4	0.553768217	0.529342997	0.897286736	0.929626595	0.727506136
5	0.55883962	0.540334129	0.88175484	0.899553723	0.720120578
6	0.668886089	0.554358472	0.863565781	0.867520154	0.738582624
7	0.701978494	0.566283142	0.85210644	0.838733525	0.7397754
8	0.71852224	0.577698392	0.818575885	0.812726417	0.731880734
9	0.768340012	0.590505999	0.800840236	0.785616777	0.736325756
10	0.776690841	0.604216707	0.776317812	0.761175433	0.729600198
11	0.785260696	0.618241398	0.728581731	0.737619348	0.717425793
12	0.789252925	0.632932625	0.700810433	0.714987936	0.70949598
13	0.810475994	0.652261596	0.674222539	0.692204442	0.707291142
14	0.823165322	0.667059517	0.662158915	0.682226613	0.708652592
15	0.835919019	0.684401451	0.645346052	0.671667794	0.709333579
16	0.835919019	0.70266915	0.635315572	0.651191394	0.706273784
17	0.848730284	0.721708639	0.612129903	0.6318461	0.703603731
18	0.848730284	0.742051786	0.593735308	0.613598084	0.699528866
19	0.861610434	0.76306033	0.59248182	0.604776192	0.705482194
20	0.874566516	0.788850174	0.585635893	0.595703506	0.711189022
21	0.887600494	0.812926391	0.574981504	0.578292022	0.713450103
22	0.900715053	0.838518519	0.572543093	0.561480162	0.718314207
23	0.900715053	0.866105585	0.557094411	0.545318465	0.717308379
24	0.918582332	0.89486166	0.548604009	0.537617958	0.72491649
25	0.936342628	0.933608247	0.537008	0.529856024	0.734203725
26	0.986159563	0.967108073	0.513772821	0.514705311	0.745436442
27	1	1	0.5	0.5	0.75

$$\mathrm{Zij} = \frac{\Delta\mathrm{Min} + \lambda\Delta\mathrm{Max}}{\Delta\mathrm{ij} + \lambda\Delta\mathrm{Max}} \begin{cases} i = 1, 2, 3 \ldots 27 \\ j, = 1, 2, 3, 4 \end{cases} \tag{6}$$

λ is the distinguishing coefficient, specified in the range $0 \leq \lambda \leq 1$ (its value can be adjusted based on the system's real requirements). is also known as the identification coefficient, and it ranges between 0 and 1. According to [26, 38, 40], $\lambda = 0.5$ is typically used since choosing 0 or 1 has no influence on the value of the parameter rankings sequence. The GRC values derived from Eq. (6) are shown in Table 7.

Stage 5: Determine the GRGi: after determining the GRCij, the GRGi may be calculated as follows Eq. (7);

$$\mathrm{GRGi} = \frac{1}{m} \sum GRCij \tag{7}$$

whereas m denotes the total number of responses (or achievement attributes) and equals 4 due to the four responses (P, H, CS, and WR). Table 7 shows the GRCs and GRGs for all experimentations that were calculated in the similar way.

Stage 6: Select the most optimally suited variable and level configurations. The higher the Grey relationship grade, the higher the product degree of excellence attribute; hence, the variable influence may be investigated, and the optimal amount level that satisfies every single one may be determined.

The GRG was stated according to [41] can be used to identify controllable components. This may be accomplished in two methods: (1) utilizing Minitab software to determine the ideal parameter configurations, or (2) manually calculating the average of the GRG scores. The procedure for finding the average GRG [42] is as follows:(1) The GRGs are grouped by variable level for each of the columns in the OA; (2) taking the average of GRGs; (3) computation of grade scores for every single L27 OA examination according to DOE.

For the purpose of quantifying the influence of variable *i*, for instance, an overall mean of grade ratings (AGV) for each level *j* is found, which is written as AGVij, and its impact, Ei, may be defined as follows:

$$\mathrm{Ei} = \mathrm{Max}\left(\mathrm{AGVij}\right)^{\circ} -^{\circ} \mathrm{Min}(\mathrm{AGVij}) \tag{8}$$

If the variable *i* can be controlled, the optimal level *j** is calculated by Eq. (8) Table 8

In the synthesis of HTMMC, the Taguchi method was utilized to compute the average grade of GRG for each level of powder metallurgy control parameters. The greater the GRG, the better the multi-achievement qualities [43]. The optimal powder metallurgy control parameters for HTMMC synthesis were milling duration (MD) level 2, compaction pressure (CP) level 2, compaction duration (CD) level 2, sintering temperature (ST) level 3, and sintering duration (SD) level 2. It may be written as MD2CP2CD2ST3SD2.

Figure 3 depicts the influence of experiment parameters on the physical and mechanical properties of HMMCs. A straight line has little effect, but a highly slanted line has a large impact on process parameters. Compaction pressure and milling duration are critical, with factors influencing their rank of impact, whereas the variables CP > MD > ST > CD > SD had an impact based on their rank of impact.

In HTMMCs materials, compaction pressure and milling time have a considerable influence on compressive strength, microhardness, and porosity. Increased CP and MD reduce porosity while improving mechanical behavior and effectiveness. The Max–Min ratio is the most important factor in powder metallurgical MMC multi-performance characteristics [27]. The final max–min value is 0.0525228, with CP and MD having the most influence on performance factors. In powder metallurgical MMC, compaction pressure and milling According to Fig. 3a, b, the optimum

Table 8 Average GRG response table

S. N	Factor of control	GRG averages by parameter levels			Max–min (*Ei*)	Rank
		L1	L2	L3		
1	Milling duration (MD)	0.7250048	0.758293	0.7139708	0.0443223	2
2	Compaction pressure (CP)	0.710134	0.762657	0.7244778	0.0525228	1
3	Compaction duration (CD)	0.7302635	0.748852	0.7181534	0.0306983	4
4	Sintering temperature (ST)	0.7274476	0.719114	0.750707	0.0315931	3
5	Sintering duration (SD)	0.721773	0.75205	0.7234459	0.0302766	5

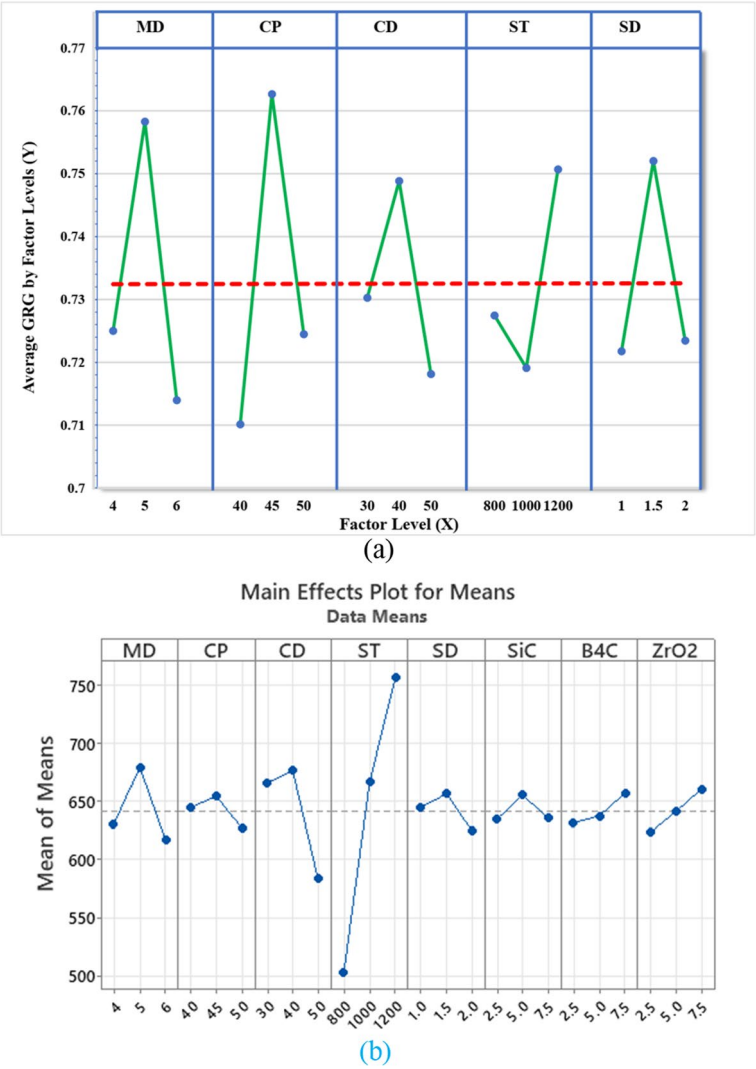

Fig. 3 **a** Main effect graph of average GRGs. **b** Main effect graph for mean from Taguchi method

outcome of process parameters and weight percentage of reinforcements: milling time 5 h, compaction pressure 45 MPa, compaction duration 40 min, sintering temperature 1200 °C, sintering temperature 1.5 h, 5%SiC, 7.5%B_4C, 7.5%ZrO_2, 4% MoS_2 for optimal sample validation experiments determined using both optimization methods.

The properties of a powder metallurgy product depend on the process parameters such as compaction pressure, sintering temperature, sintering time, type and rate of reinforcement, size of matrix and reinforcing elements, etc. [45]. Homogeneity in powder mixing, compaction pressure, and sintering temperature is critical for producing samples with higher mechanical qualities for novel HTMMCs required for engineering applications, including matrix and reinforcement weight percentages and attributes. The reinforcement and matrix weight percentage compositions were previously established in line with the experimental design employed in this study. Following optimization, the optimal sample weight percentage was used directly in this validation experiment.

Powder metallurgy was mixed and combined reinforcing and matrix elements to create a green compact. The compacts are compressed at a certain pressure based on the required porosity. The green compacts are then heated to high temperatures to promote diffusion bonding. This process is called sintering, and the most important factors are the compaction pressure, holding temperature, and holding duration. These characteristics have a significant impact on the qualities of powder metallurgical products. Reinforcement materials have a substantial impact on composite material qualities since they are determined by the type and bonding of reinforcement materials to the matrix material. The % weight fraction of reinforcing materials is critical for manufacturing. The law of mixing determines the attributes of a composite material, which are always intermediate between the properties of the component elements [46].

Validation experimentations

The validation test for HTMMCS, a material used in biomedical equipment, vehicles, and aircraft components, used optimal process parameters, reinforcement, and matrix to investigate wear rate, porosity, Rockwell hardness, and compressive strength. The results validated TGRA's efficacy in multi-output optimization, predicting physic mechanical characteristics. The optimization technique is viable for developing innovative structural materials with improved experimental findings, demonstrating the material's potential for usage in a variety of applications. Figure 4 shows a digital display of experimental data from a Rockwell hardness type "C" testing equipment. Table 9 shows the improved process parameters, matrix, and reinforcements as a percentage of prior experimentally observed data. The validation examination findings generated by the confirmation test are shown in Table 10.

Microstructure analysis

Figure 5 exhibits micrographs illustrating the samples taken from an SEM shown below. SEM was used to examine the surface morphology of TMMC and base-Ti6Al4V specimens for themselves, exhibiting a coarse lamellar + morphology associated separation of

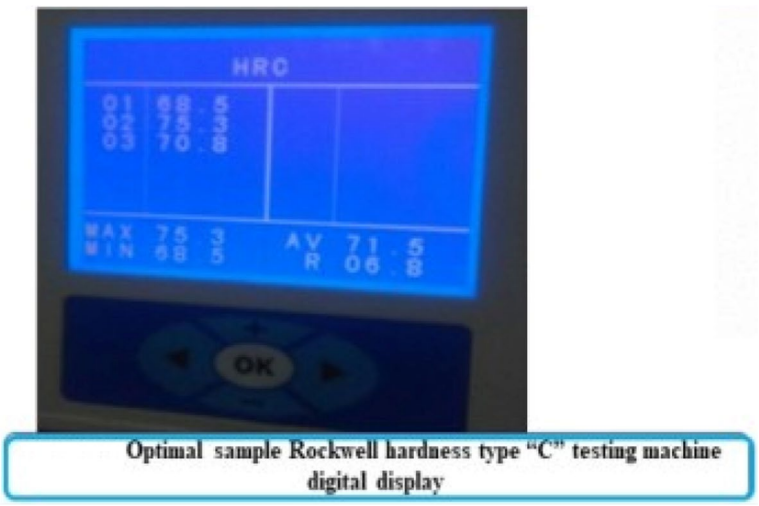

Fig. 4 Optimal sample Rockwell hardness type "C" testing machine digital display

Table 9 Optimal variable configuration for HTMMCs synthesis

S. N	Milling time	Compaction pressure	Compaction time	Sintering temperature	Sintering time	SiC	B_4C	ZrO_2	MoS_2	Ti
	(h)	(MPa)	(min)	(^{0}C)	(h)	%	%	%	%	%
OS	5	45	40	1200	1.5	5	7.5	7.5	4	76%

Table 10 Validation examination outcomes

S. N	Validation examination outcomes	Measured responses data			
		Trial-1	Trial-2	Trial-3	Average response value
1	Wear rate (WR) (mm^3)	0.1972	0.1823	0.1834	0.18763
2	Porosity(P) (%)	0.1209	0.1116	0.1209	0.1178
3	Compressive strength (CS) (MPa)	2810.89	2782	2754.18	2782.36
4	Rockwell hardness type "C" RBN)	68.5	75.3	70.8	71.53

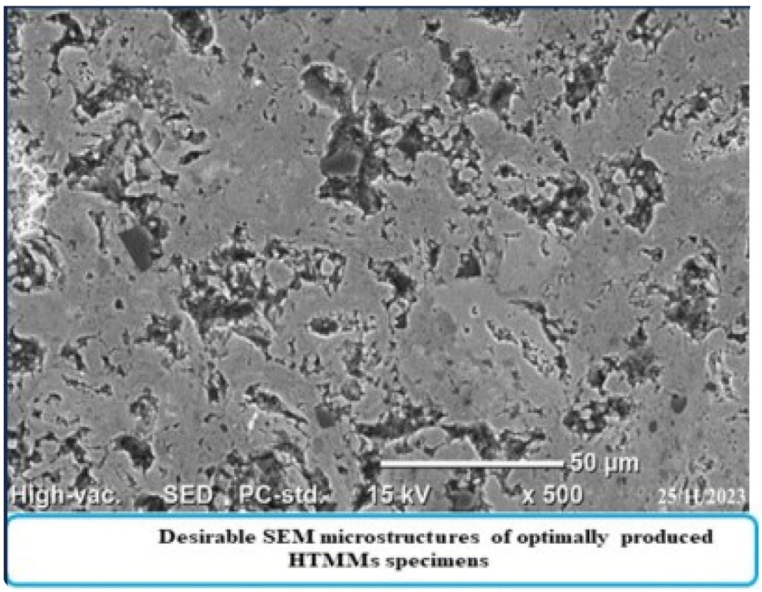

Fig. 5 Desirable SEM microstructures of optimally produced HTMMs specimens

phases at elevated temperature sintering and consequently sluggish rate of cooling [33]. SEM micrographs indicate that raising the percentages of ZrO_2 and B_4C, decreasing SiC, and inserting MoS_2 particles into a Ti-based metal matrix reduces porosity and densifies the surface. In the produced sample SEM morphology observed in micrographs, ZrO2 reinforcement creates and source of agglomerations.

The insertion of course, columnar grains into a fine-grained microstructure would not be expected to improve mechanical strength; in fact, the most likely impact would be for that section of the component to lose strength [47]. Optimum specimen (OS) has lower porosity boundaries between reinforcement particles and phases, and porosity rises as the number of reinforced particles increases.

XRD analysis

XRD with Bragg's law and a computerized powder X-ray diffractometer were used to analyze the elemental phases in manufactured samples. Miller indices were utilized to distinguish between atom planes and diffraction peaks. The phases were identified using ASTM X-ray diffraction data cards. Minor precipitate stages were personally validated and compared using JCPDS cards.

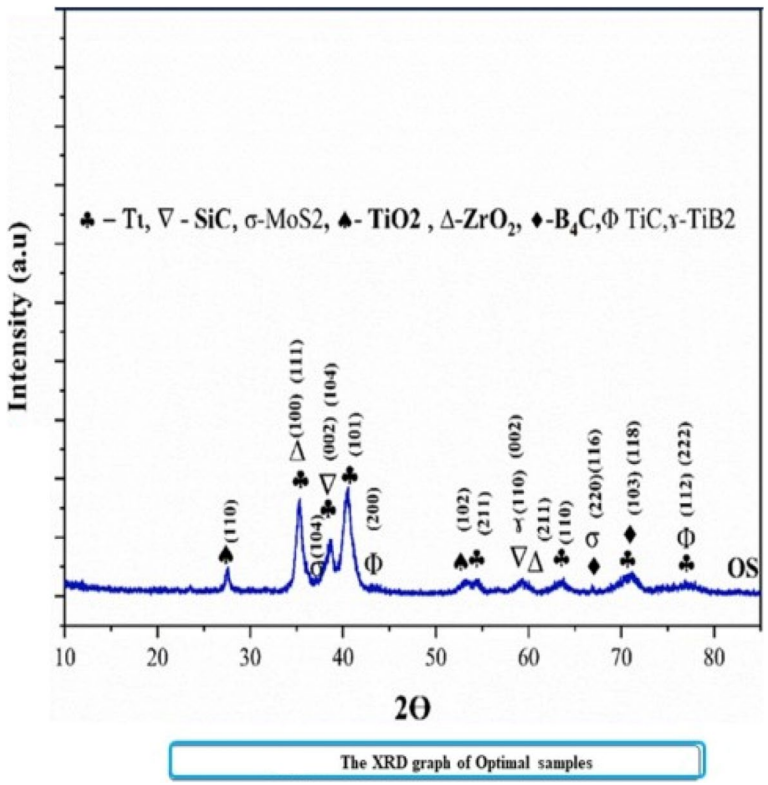

Fig. 6 The XRD graph of optimal samples

Figure 6 shows an XRD pattern of HTMMCs composite powders milled prior to compaction and sintering, suggesting a strong interfacial chemical interaction between hybrid reinforcements. The hexagonal tightly packed crystal structure of the titanium grade 5 matrix samples has a density of 4.43 g/cm^3. The existence of Ti, SiC, B_4C, MoS_2, ZrO_2, and rutile (TiO_2) in the titanium metal matrix is connected to the presence of these phases. The B_4C interacted mostly with the Ti of the substrate as follows [19, 44]: Due to the fact that $5Ti + B_4C = TiC + 4TiB$, in rare cases TiC maxima can also be discovered at $2\Theta = 41.6^{\circ}$, 44°, and 76.0° angles, which coincide to crystal orientation (2000) and (222). TiB peaks (JCPDS: 0044598) may be found at $2\Theta = 58.8^{\circ}$ position orientations. As a result of this reaction, TiB and TiC phases are produced in the composite, as evidenced by XRD data. Because of the great hardness of the ceramics, this new phase has significantly improved the mechanical properties of synthesized optimal samples.

Conclusions

Titanium grade 5 MMCs were used to manufacture a Ti–B_4C–SiC–MoS_2–ZrO_2 nanocomposite for automotive and aerospace applications. The composites had a more desirable microstructure and enhanced particle dispersion homogeneously. The increase of reinforcement material lowered the wear rate, and matrix interfacial contact and adhesion impacted composite strength. The end effect is reduced porosity and wear rate while boosting Rockwell microhardness and compressive strength. The following are the manuscript's final remarks:

1. The milling time was the most important parameter than ST, CP, SD, and CT which had a lesser impact. The increased compaction pressure resulted in decreased porosity and enhanced material behavior.
2. The optimal levels' settings of powder metallurgy control parameters in the synthesis of HTMMC control factors were milling duration (MD) at level 2 used 5 h, compaction pressure (CP) at level 1 used at 40 MPa, compaction duration (CD) at level 2 used 40 min, sintering temperature (ST) at level 3 used 1200 °C temperature, and sintering duration (SD) at level1 used 1 h. It may be stated simply as MD2CP-1CD2ST3SD1.
3. The average density, porosity, hardness, compressive strength, and wear rate of 4.29 gm/cm^3, 0.1178%, 71.53 RHN, 2782.36 MPa, and 0.1519 mm^3 respectively have been obtained at optimal parameter settings. The study concludes that
4. The best outcomes are achieved by HTMMC material created at the determined optimum parameter values.

The dry sliding wear is investigated using a POD with load, sliding distance, and velocity parameters. It discovers that matrix materials have a homogeneous particle distribution, with nanoparticles such as B_4C, SiC, ZrO_2, and MoS_2 playing important roles in WR values. Composites produced with increased hardness have a reduced wear rate. Titanium grade 5 combines with reinforcements to produce TiB_2 and TiC, which improves hardness and compressive HTMMCS. The results of XRD and SEM demonstrate that matrix interfacial contact and adhesion have a direct influence on composite strength.

Abbreviations

TGRA	Taguchi-based Grey relational analysis
HTMMCs	Hybrid titanium metal matrix composites
MMCs	Metal matrix composites
TMMCs	Titanium metal matrix composites
PM	Powder metallurgy
POD	Pin on disc
CP	Compaction pressure
MD	Milling duration
CD	Compaction duration
SD	Sintering duration
OS	Optimum specimen
S/N	Signal-to-noise ratio
SEM	Scanning electron microscope
X-RD	X-ray diffraction

Acknowledgements
Not applicable.

Authors' contributions
Every author has significant contribution to the research work. All authors have read and approved the manuscript.

Funding
No funding has been given for this research work.

Availability of data and materials
The datasets used and/or analyzed during the current study are available from the corresponding author on reasonable request.

Declarations

Competing interests
The authors declare that they have no competing interests.

Received: 13 January 2024 Accepted: 8 April 2024
Published online: 04 July 2024

References

1. Siengchin S (2023) A review on lightweight materials for defence applications: Present and future developments. Def Technol 24:1–17. https://doi.org/10.1016/j.dt.2023.02.025
2. Khanna N, Zadafiya K, Patel T, Kaynak Y, Rashid RAR, Vafadar A (2021) Review on machining of additively manufactured nickel and titanium alloys. J Market Res 15:3192–3221
3. Abd-Elwahed MS, Ibrahim AF, Reda MM (2020) Effects of ZrO2 nanoparticle content on microstructure and wear behavior of titanium matrix composite. J Market Res 9(4):8528–8534
4. Penyashki T, Kamburov V, Kostadinov G, Kandeva M, Dimitrova R, Nikolov A (2021) Some ways to increase the wear resistance of titanium alloys. J Balk Tribol Assoc 27(1):1–20
5. Chirico C, Romero AV, Gordo E, Tsipas SA (2022) Improvement of wear resistance of low-cost powder metallurgy β-titanium alloys for biomedical applications. Surf Coat Technol 434:128207
6. Gisario A, Kazarian M, Martina F, Mehrpouya M (2019) Metal additive manufacturing in the commercial aviation industry: a review. J Manuf Syst 53:124–149
7. Chen T, Koyama S, Nishida S, Yu L (2021) Mechanical properties and frictional wear characteristic of pure titanium treated by atmospheric oxidation. Materials 14(12):3196
8. Saurabh A, Meghana CM, Singh PK, Verma PC (2022) Titanium-based materials: synthesis, properties, and applications. Materials Today: Proceedings 56:412–419
9. Shi X, He P, Sun S, Chen J, Beake BD, Liskiewicz TW, Zhou Z (2022) Tailoring the corrosion and tribological performance of Ti-modified MoS2-based films in simulated seawater. J Mater Res Technol. 21:576–89
10. Gonçalves VRM, Corrêa DRN, Grandini CR, Pintão CAF, Afonso CRM, LisboaFilho PN (2023) Assessment of improved tribocorrosion in novel in-situ Ti and β Ti–40Nb alloy matrix composites produced with NbC addition during arc-melting for biomedical applications. Mater Chem Physics. 301:127597
11. Sharma AK, Bhandari R, Aherwar A, Rimašauskienė R (2020) Matrix materials used in composites: A comprehensive study. Materials Today: Proceedings 21:1559–1562
12. Zhang X, Li D, Zheng Y, Shojaei P, Trabia M, O'Toole B, Liao Y (2022) In-situ synthesis of Ti5Si3-reinforced titanium matrix nanocomposite by selective laser melting: Quasi-continuous reinforcement network and enhanced mechanical performance. J Mater Process Technol. 309:117752
13. Shalnova SA, Volosevich DV, Sannikov MI, Magidov IS, Mikhaylovskiy KV, Turichin GA, Klimova-Korsmik OG (2022) Direct energy deposition of SiC reinforced Ti–6Al–4V metal matrix composites: Structure and mechanical properties. Ceram Int 48(23):35076–35084
14. Dong ZW, Xia Y, Guo XY, Liu HN, Liu PD (2022) Preparing low-oxygen Ti-6Al-4V alloy powder through direct reduction of oxides and its synergistic reaction mechanism. Journal of Central South University 29(6):1811–1822
15. Liu L, Zhang H, Cheng X, Mu X, Fan Q (2022) Graphene nanoplatelets induced laminated heterogeneous structural titanium matrix composites with superior mechanical properties. Ceram Int 48(24):37470–37475
16. Kumar D, Pandey KK, Kumari S, Nair AM, Mirche KK, Maurya SS, Keshri AK (2022) Effect of nanodiamond concentration on the electrochemical behavior of plasma sprayed titanium-nanodiamond nanocomposite coatings. Diamond Relat Mater. 130:109419
17. Vairamuthu J, Kumar AS, Sivakumar GD, Navroz SN, Kailasanathan C (2022) Mechanical properties of casting titanium alloy matrix composites reinforced by WC and TiB2 ceramic particulates. Materials Today: Proceedings 59:1503–1507
18. Oke SR, Falodun OE, Okoro AM, Tshephe TS, Olubambi PA (2019) Effect of ZrO2 addition on densification and properties of Spark plasma sintered Ti6Al4V-Ni. Materials Today: Proceedings 18:2454–2460
19. Guo S, Li Y, Gu J, Liu J, Peng Y, Wang P, Wang K (2023) Microstructure and mechanical properties of Ti6Al4V/B4C titanium matrix composite fabricated by selective laser melting (SLM). J Mater Res Technol. 23:1934–1946
20. Chen XW, Li ML, Zhang DF, Cai LP, Ren P, Hu J, Liao DD (2022) Corrosion resistance of MoS2-modified titanium alloy micro-arc oxidation coating. Surf Coat Technol 433:128127
21. Li S, Wang X, Wei Z, Han Y, Shi H, Le J, Lu W (2022) Simultaneously improving the strength and ductility of the as-sintered (TiB+ La2O3)/Ti composites by in-situ planting ultra-fine networks into the composite powder. Scripta Materialia. 218:114835
22. Feng Z, Duan Y, Cao Y, Qi H, Peng M, Wang X (2023) Corrosion properties of ceramic coating on pure titanium by pack boronizing with Nd2O3. Ceramics International. 49(10):15101–13
23. Okoro AM, Machaka R, Lephuthing SS, Awotunde MA, Oke SR, Falodun OE, Olubambi PA (2019) Dispersion characteristics, interfacial bonding and nanostructural evolution of MWCNT in Ti6Al4V powders prepared by shift speed ball milling technique. J Alloy Compd 785:356–366
24. Zaki MU, Hussain S (2021) Impact of addition of manganese and boron carbide on aluminium metal matrix composites using powder metallurgy process. Materials Today: Proceedings 44:4364–4368
25. Manohar G, Pandey KM, Maity SR (2021) Effect of compaction pressure on mechanical properties of AA7075/B4C/graphite hybrid composite fabricated by powder metallurgy techniques. Materials Today: Proceedings 38:2157–2161
26. Ikubanni PP, Oki M, Adeleke AA, Agboola OO (2021) Optimization of the tribological properties of hybrid reinforced aluminum matrix composites using Taguchi and Grey's relational analysis. Scientific African 12:e00839
27. Ashebir DA, Mengesha GA, Sinha DK, Bereda YB (2022) Multi-response optimization of process and reinforcement parameters of hybrid reinforced Al matrix composites using Taguchi-Grey relational analysis. Engineering Research Express 4(4):045038
28. Kamalizadeh S, Niknam SA, Balazinski M, Turenne S (2022) The use of TOPSIS method for multi-objective optimization in milling Ti-MMC. Metals 12(11):1796

29. Ramadoss N, Pazhanivel K, Ganeshkumar A, Arivanandhan M (2022) Effect of SiC and MoS2 Co-reinforcement on enhancing the tribological and anti-corrosive performance of aluminum matrix (Al6063-T6) nanocomposites. SILICON 14(10):5471–5479
30. Sharma DK, Mahant D, Upadhyay G (2020) Manufacturing of metal matrix composites: a state of review. Materials Today: Proceedings 26:506–519
31. Freschi M, Arrigoni A, Haiko O, Andena L, Kömi J, Castiglioni C, Dotelli G (2022) Physico-mechanical properties of metal matrix self-lubricating composites reinforced with traditional and nanometric particles. Lubricants 10(3):35
32. Pérez-Soriano EM, Montealegre-Meléndez I, Arévalo Mora CM, Kitzmantel M, Neubauer E (2022) Comparative study of the behaviour of several reinforcement materials in titanium matrix produced by Rapid Sinter Pressing Manufacturing. Revista de Metalurgia. 58(4):229
33. Gemeda BA, Sinha DK, Singh GK, Alghtani AH, Tirth V, Algahtani A, Hossain N (2022) Effect of sintering temperatures, reinforcement size on mechanical properties and fortification mechanisms on the particle size distribution of B4C, SiC and ZrO2 in titanium metal matrix composites. Materials. 15(16):5525
34. Gerus-Gosciewska M, Gosciewski D (2022) Grey relational analysis (GRA) as an effective method of research into social preferences in urban space planning. Land 11(1):102
35. Prakash JU, Rubi CS, Rajkumar C, Juliyana SJ (2021) Multi-objective drilling parameter optimization of hybrid metal matrix composites using grey relational analysis. Materials Today: Proceedings 39:1345–1350
36. Joshi MP, Singh J, Prakash C, Singh S (2019) On the multi-parametric optimization of quality characteristics of the hybrid Al-6061 composites fabricated through powder metallurgy. In IOP Conference Series: Materials Science and Engineering. 561(1):012053 (IOP Publishing)
37. Achuthamenon Sylajakumari P, Ramakrishnasamy R, Palaniappan G (2018) Taguchi grey relational analysis for multi-response optimization of wear in co-continuous composite. Materials 11(9):1743
38. Poornesh M, Bhat S, Gijo EV, Bellairu PK, McDermott O (2022) Multi-response modelling and optimisation of mechanical properties of Al-Si alloy using mixture design of experiment approach. Processes 10(11):2246
39. Julong D (1989) Introduction to grey system theory. J Grey Syst 1(1):1–24
40. Naqiuddin NH, Saw LH, Yew MC, Yusof F, Poon HM, Cai Z, San Thiam H (2018) Numerical investigation for optimizing segmented micro-channel heat sink by Taguchi-Grey method. Appl Energy 222:437–450
41. Haq AN, Marimuthu P, Jeyapaul R (2008) Multi response optimization of machining parameters of drilling Al/SiC metal matrix composite using grey relational analysis in the Taguchi method. Int J Adv Manuf Technol 37:250–255
42. Bodunrin MO, Alaneme KK, Chown LH (2015) Aluminium matrix hybrid composites: a review of reinforcement philosophies; mechanical, corrosion and tribological characteristics. J Market Res 4(4):434–445
43. Shaikh IA, Rao MV (2015) A Review on optimizing process parameters for TIG welding using taguchi method & grey relational analysis. Int J Sci Res 4(6):2449–2452
44. Li R, Yue H, Luo S, Zhang F, Sun B (2023) Microstructure and mechanical properties of in situ synthesized (TiB+ TiC)-reinforced Ti6Al4V composites produced by directed energy deposition of Ti and B4C powders. Mater Sci Eng, A 864:144466
45. Kumar N, Bharti A, Dixit M, Nigam A (2020) Effect of powder metallurgy process and its parameters on the mechanical and electrical properties of copper-based materials: Literature review. Powder Metall Met Ceram 59:401–410
46. Kumar N, Bharti A, Saxena KK (2021) A re-investigation: effect of powder metallurgy parameters on the physical and mechanical properties of aluminium matrix composites. Materials Today: Proceedings 44:2188–2193
47. Barrie C, Fernandez-Silva B, Snell R, Todd I, Jackson M (2023) AddFAST: A hybrid technique for tailoring microstructures in titanium-titanium composites. J Mater Process Technol 315:117920

Publisher's Note